Analysis of Time Delay Effects for Wide-Area Damping Control Design using Dominant Path Signals

Yuwa Chompoobutrgool, *Student Member, IEEE*, and Luigi Vanfretti, *Member, IEEE*

***Abstract*—The purpose of this article is to investigate the effects of time delays for wide-area damping control design when signals from *dominant inter-area oscillation paths* are used as feedback inputs for damping controllers. The analysis is carried out using a two-area study system. Frequency and time-domain responses of a generator's terminal voltage when the PSS uses PMU signals subject to time delays will be compared and assessed. The analysis reveals that while modal observability of the dominant path signals corresponds to the gain of the open-loop system at the inter-area frequency, these properties are inversely proportional to their corresponding delay margins.**

***Index Terms*—Time delays, synchronized phasor measurements, wide-area damping control, dominant inter-area oscillation paths.**

I. Introduction

TIME delays have an impact on control loops [1] and may affect overall power system stability. In the past, the delays were often ignored since the controls were usually fed by local feedback signals. However, being driven by the concept of Wide-Area Control Systems (WACS), more recent research have included time delays in power system studies. Several works on damping control suggest that wide-area control may be more effective than local control due to the lack of observability of certain inter-area oscillations in local measurements [2]. Furthermore, previous studies in feedback control show that time delays cause (1) destabilizing effects, (2) degradation of the controller's performance, and (3) loss of synchronism [3]. As such, to implement PMU measurements for wide-area damping control (WADC), time delays, together with their impacts on control performance and system stability, must be carefully investigated.

One relevant issue regarding WADC besides time delay considerations in control design is the selection of feedback input signals for damping controllers. The conventional input signal for power system stabilizers (PSS), the most commonly used damping controller, is generator rotor speed which is locally available. With the presence of PMUs, more choices of feedback signals, i.e. wide-area or remote ones, become available. Among these PMU signals[1], [4], [5] present a systematic approach using the concept *dominant inter-area oscillation paths*[2] to select feedback input signals having highest open-loop observability. The assumption is that using signals from the dominant paths as controller feedback inputs, more effective damping performance can be achieved compared to using any other signals within the network. Moreover, the network modeshapes[3] of the dominant path signals indicate damping effectiveness, i.e. the larger the network modeshape a signal has, the higher damping ratio the system can achieve [6].

To date, several studies have considered time delay in damping control design using different algorithms [2], [3], [7]. Nevertheless, some important aspects such as analyses on the impacts of the delay on the properties of feedback input signals have not yet been investigated. As such, the purpose of this article is to investigate the effects of time delays when signals from dominant paths are used as feedback inputs.

The paper is organized as follows. In Section II, modelling of the study system and time delays is described. Section III presents the analysis of time delay impacts on input signal feedback properties using dominant path signals, while in Section IV further analysis is carried out using nonlinear time-domain simulations. Conclusions are presented in Section V.

II. Power System Modelling

In [6] it has been shown that the damping performance of a feedback signal corresponds to the amount of its inter-area modal content. That is, the larger the modal content a signal has (when used as feedback inputs to the damping controller), the higher damping ratio the system achieves. In an interconnected system, [4] and [5] propose that signals from *dominant inter-area oscillation paths* have the highest content of the inter-area modes of interest. Therefore, they should be used as feedback inputs for damping controllers such as PSSs.

A. Study System

The system of study is illustrated in Fig. 1 where G_1 and G_2 represent the main clusters of machines involved in the inter-area swing while transformers and line impedances represent elements of the dominant path connecting the two areas. The inter-area mode of the system is $-0.0360 \pm j2.6104$, which has a frequency and damping ratio of 0.4154 Hz and 1.38 %, respectively[4].

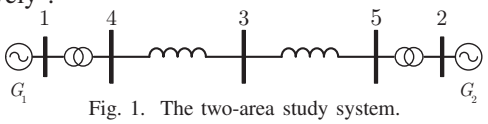

Fig. 1. The two-area study system.

Y. Chompoobutrgool and L. Vanfretti are with KTH Royal Institute of Technology, Stockholm, Sweden. E-mail: yuwa@kth.se, luigiv@kth.se

L. Vanfretti is with Statnett SF, Research & Development, Oslo, Norway. E-mail: luigi.vanfretti@statnett.no

Y. Chompoobutrgool is supported by Elforsk, Sweden. L. Vanfretti is supported by Statnett SF and the STandUP for Energy collaboration initiative.

[1]Voltage and current phasors, i.e. voltage and current magnitude and angles.

[2]These paths are defined as the passageways containing the highest content of inter-area oscillations.

[3]The modal observability of the network signals, e.g. voltage and current phasors. In this study, only the voltage magnitude and voltage angles are considered.

[4]Refer to [6] for further details of the study system.

978-1-4799-6415-4/14/$31.00 ©2014 IEEE

B. Simulation Approach

The study system is modeled using the Power System Analysis Toolbox (PSAT) [8]. After linearization, the A, B, C, and D matrices are implemented in MATLAB/Simulink where frequency-domain and linear time-domain analyses are carried out. The damping controller includes a PSS (which is installed at G_1), a washout filter, and/or a torsional filter (active when input signals are voltage angles or speed). A time delay block is included in the feedback path of the control loop. The feedback input signals of interests are voltage magnitudes and voltage angle differences along the dominant path of the study system. The block diagram of the closed-loop system with a PSS and time delay is depicted in Fig. 2. For the nonlinear time-domain analysis, PSAT's time-domain simulation routine is used.

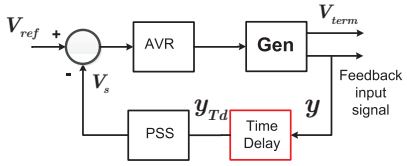

Fig. 2. Block diagram representative of the study system.

C. Time Delay Modelling and Software Implementation

In this study, the time delay is modeled using a 2^{nd}-order Padé approximation. This delay represents an end-to-end delay which is comprised by communication network delays and signal processing delays in the WACS system.

Since there is no delay model in PSAT, the 2^{nd}-order Padé approximation was implemented in the software by adding the transfer function

$$TD(s) = \frac{12 - 6sT_d + T_d^2 s^2}{12 + 6sT_d + T_d^2 s^2} \tag{1}$$

within a PSS class where T_d represents time delay in seconds. This transfer function corresponds to two differential equations:

$$\dot{x}_1 = x_2 \tag{2}$$

$$\dot{x}_2 = -\frac{12}{T_d^2}x_1 - \frac{6}{T_d}x_2 + V_{SI} \tag{3}$$

where x_1 and x_2 represent time delay's state variables and V_{SI} represents an input signal[5].

III. Feedback Property Analysis of Dominant Path Signals Considering Time Delays

The linearized model of the study system is used in this analysis. Signals V_3 and $\Delta\theta_{45}$ are used as feedback inputs for representing voltage magnitude and voltage angle differences, respectively. PSS parameters are designed using the same method as in [6].

[5]See [9] for details on how to implement a device in PSAT.

A. Impact on Frequency Responses

The frequency responses, namely root locus and bode plots, of the open-loop system at y_{Td} (see Fig. 2) for varying time delays are illustrated in Figs. 3 - 4, respectively. Fig. 5 illustrates the root locus plots of the open-loop system at V_s for varying time delays using a fixed PSS. 'x' mark denotes the point where the fixed gain K_d is 0.000503 for each closed-loop system. Damping ratios corresponding to these points together with changes in phases measured at the inter-area frequency (*PIF*) and the angles of departure (θ_{dep}) are summarized in Table I.

It is shown that time delays result in a reduction of the angles of departure and phase lag, and, more importantly, degradation of damping performance. For every 100 ms, the phase is lagged by about 15° at the inter-area frequency. Thus, the larger the delay, the more phase compensation is needed.

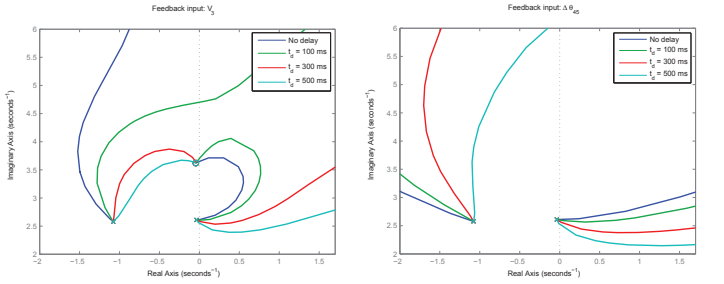

(a) Voltage Magnitude, V_3 (b) Voltage Angle Difference, $\Delta\theta_{45}$

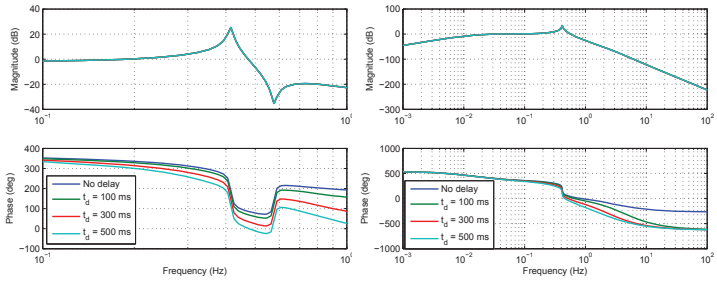

(a) Voltage Magnitude, V_3 (b) Voltage Angle Difference, $\Delta\theta_{45}$

Fig. 4. Bode plots for varying time delays.

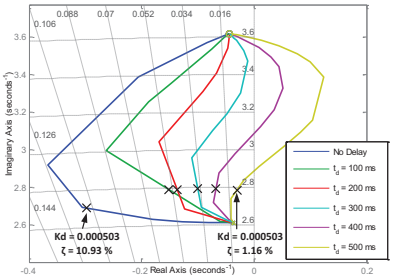

Fig. 5. Root Locus plots for varying time delays, including PSS.

TABLE I
Control Loop Metrics at Different Time Delays when V_3 is used as Feedback Input.

T_d (ms)	*PIF* (deg)	θ_{dep} (deg)	ζ (%)
0	-170.99	9.61	10.93
100	-185.95	-4.59	8.46
200	-200.90	-18.85	6.29
300	-215.84	-33.20	4.37
400	-230.73	-47.64	2.67
500	-245.50	-62.20	1.16

B. Impact on Time Responses

A 1% step change is applied at the voltage reference, V_{ref}, of the exciter (see Fig. 2). The time responses of the generator's terminal voltage, V_1, for different delays are illustrated in Fig. 6. It can be seen that as time delay increases, responses of the terminal voltages oscillate more and exhibit a phase lag. Comparing between Fig. 6a and 6b, the same amount of time delays yield different impact on different input signals.

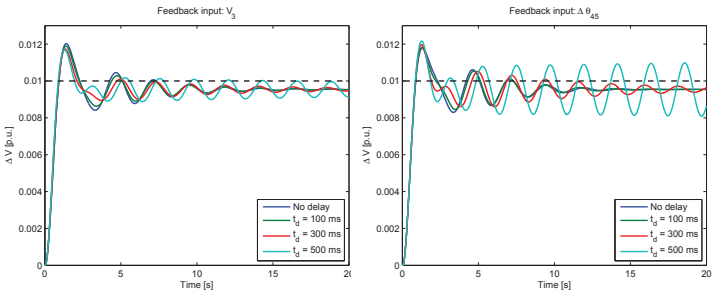

(a) Voltage Magnitude, V_3 (b) Voltage Angle Difference, $\Delta\theta_{45}$

Fig. 6. Time responses after a step change.

C. Comparison Among Dominant Path Signals

Dominant path signals referred in this study are voltage magnitudes and voltage angles at Bus 1, 4, 3, 5, and 2 (the order follows the diagram in Fig. 1). For voltage angle signals, the differences between two buses are used where Bus 4 is chosen as the reference.

Fig. 7 shows the Bode plots of the open-loop system measured at y (see Fig. 2), when different signals are implemented as feedback inputs. Note that T_d = 0 s in this case. Angles of departure, gain and phase of the open-loop system measured at inter-area frequency, (denoted by *GIF* and *PIF*, respectively) and delay margins are summarized in Table II and Table III for voltage magnitude and voltage angle differences, respectively. Note that the term *delay margin* (DM) is defined as the smallest time (for $T_d > 0$) required to destabilize the closed-loop system[6].

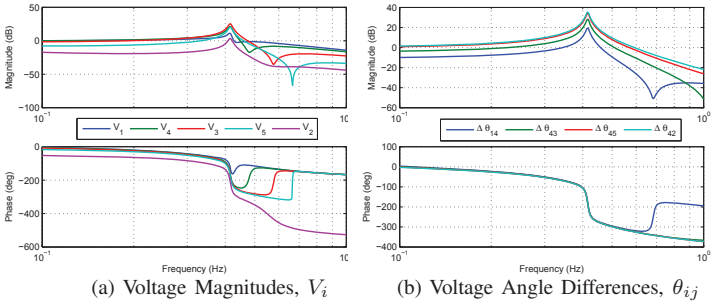

(a) Voltage Magnitudes, V_i (b) Voltage Angle Differences, θ_{ij}

Fig. 7. Bode plots of different feedback inputs, no delay.

[6]See [10] for details on the computation of delay margin.

TABLE II
CONTROL LOOP METRICS AT THE INTER-AREA FREQUENCY AND DELAY MARGINS WHEN V_i IS USED AS FEEDBACK INPUT.

Signal	θ_{dep} (deg)	*GIF* (dB)	*PIF* (deg)	DM (ms)
V_1	36.70	3.56	-131.77	1750
V_4	15.41	11.85	-164.23	756
V_3	9.61	18.52	-170.99	587
V_5	4.16	10.49	-175.59	646
V_2	-34.87	1.51	-212.76	N/A [7]

TABLE III
CONTROL LOOP METRICS AND DELAY MARGINS WHEN $\Delta\theta_{ij}$ IS USED AS FEEDBACK INPUT.

Signal	θ_{dep} (deg)	*GIF* (dB)	*PIF* (deg)	DM (ms)
θ_{14}	7.43	9.45	-179.48	1017
θ_{43}	3.81	25.67	-181.27	634
θ_{45}	2.30	50.23	-182.13	494
θ_{42}	6.32	58.74	-182.53	457

Recall the dominant path properties in [4], voltage magnitude modeshapes, S_V, are largest at the center of the path and smallest at both edges while, on the other hand, voltage angle modeshapes, S_θ, are largest at both edges but in opposite directions and smallest at the center. The results in [6] demonstrate that the damping performance correspond to the magnitude of the network modeshape. The larger the network modeshape of a signal, the higher the damping performance becomes.

From the results in Table II - III, important relationship between certain properties and the dominant path signals can be deduced:

- Angles of departure θ_{dep} and phase of the open-loop systems measured at the inter-area frequency are proportional to the electrical distance from the controller.
- S_V and S_θ are proportional to gain of the open-loop systems measured at the inter-area frequency.
- S_V and S_θ are inversely proportional to the delay margin.

Angles of departure and/or phase measured at the inter-area frequency determine how much phase compensation a controller requires. The closer the signal along the dominant path to the compensation is needed. However, the damping capacity is determined by the gain measured at the inter-area frequency which is the factor that can be raised before instability arises [11]. The larger the *GIF*, the higher the damping capacity a signal has.

Hence, there is a trade-off to assess when selecting feedback input signals. While the dominant path signals with highest observability (S_V, S_θ) (thus the highest damping capacity) have the largest *GIF*, they have the lowest delay margin. Therefore, the trade-off between damping efficacy and actual latency of a controller needs to be taken in to account.

To verify the computed delay margin, T_d = 587 ms is applied to the system with V_3 as feedback input signal. The corresponding time responses to a step change and the Bode plot are illustrated in Fig. 8. It can be seen from Fig. 8a that the responses are marginally stable. This can also be confirmed

[7]The gain plot of this system does not cross any point where the gain margin is equal to 0 dB, thus no gain crossover frequency (ω_g) can be computed. Since DM is computed at the ω_g, DM is not available in this case.

by Fig. 8b where the the phase margin of the system including delay $(G(s)+PSS(s)+TD(s))$ is $-180°$ at the gain crossover frequency.

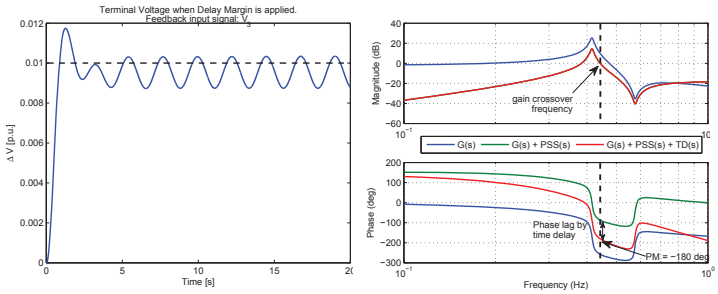

(a) Time response after a step change. (b) Bode plot

Fig. 8. Verification of Delay Margin: Linearized system.

Next, responses considering a fixed time delay of 200 ms when different dominant path signals are used as feedback inputs are analyzed. The same PSS is applied to all feedback inputs of the same type. Time responses of the linearized system after a 1% step change at V_{ref} are demonstrated in Fig. 9. For the same amount of delay, the damping performance corresponds to each signal's respective network modeshape (S_V, S_θ). In other words, the larger the network modeshape, the larger the damping is. (See [6] for computations of damping performance for each feedback input signal.)

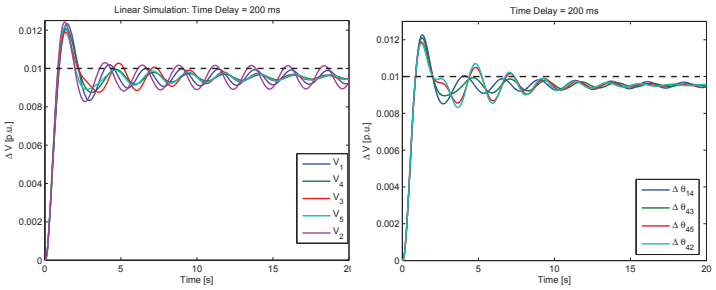

(a) Voltage Magnitude, V_i (b) Voltage Angle Differences, $\Delta\theta_{ij}$

Fig. 9. Time responses after a step change, time delay = 200 ms.

IV. Verification of the Results through Non-Linear Time-Domain Simulations

The results obtained from linear analysis in the previous section will be validated with nonlinear time-domain simulations using PSAT. Note that only the results using the voltage magnitude as feedback input signal will be illustrated here.

A. Closed-Loop Responses subject to Delays

Keeping the same feedback input signals and PSS parameters, the same time delays as implemented in Section III are applied to the study system. To illustrate the shifts caused by time delays, the output from the PSS is shown in Fig. 10a. The responses at the terminal voltages to varying time delays using V_3 as feedback signal are shown in Fig. 10b. Similar to the linear results in Fig. 6a, as time delay increases, the responses shift further to the right (phase lags) and the oscillation becomes larger.

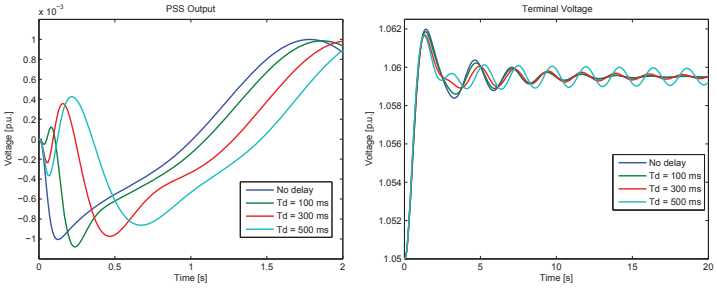

(a) PSS Output Signal (b) Terminal Voltages, V_1

Fig. 10. Responses subject to different time delays of (a) PSS output and (b) Terminal Voltage, V_1.

B. Verification of Delay Margins

To validate if the delay margin computed from the linearized system will exhibit the same behavior during nonlinear time-domain simulations, the same delay margin (DM = 587 ms), together with the same perturbation, is applied to the study system. The time-domain response is compared with the linear response in Fig. 11. While the linear response is marginally stable, the nonlinear response is, though inconspicuously, unstable. Although not shown here, the delay that makes the nonlinear system marginally stable is at 580 ms. This implies that the delay margin obtained from the linear model response requires $\pm$ 10 ms correction of the margin.

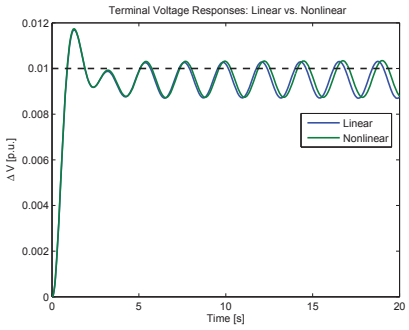

Fig. 11. Terminal Voltages, V_1, DM = 587 ms.

C. Comparison Among Dominant Path Signals

Time delay of 200 ms is applied to the system with the same perturbation and using the same PSS as in the linear simulation. Nonlinear time-domain responses to different dominant path signals are shown in Fig. 12. Despite some small variations, the responses and damping performance correspond to the linearize

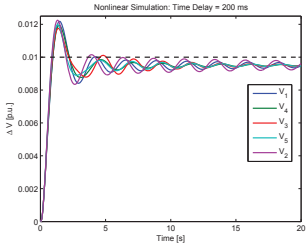

Fig. 12. Voltage Magnitude, V_i

D. Nonlinear Disturbance & Time Delay Compensation

To simulate how the system will react to a large disturbance and delays, a fault is applied at Bus 5 for 125 ms. The responses after the disturbance when no PSS is used, when PSS is implemented and when PSS is implemented with a

time delay of 250 ms are illustrated in Fig. 13 in black, red, and blue traces, respectively. Note that V_3 is used as feedback input signal and its corresponding PSS parameters are tuned. It can be seen that time delays not only result in a shift of the responses but also degrade the controller's damping performance.

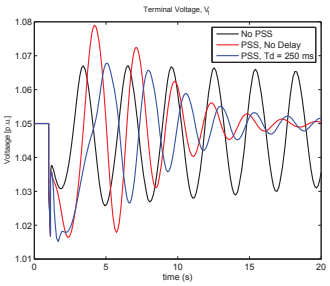

Fig. 13. Responses after disturbances, no delay compensation.

To compensate for the delay, a single-stage phase lead block is added after the PSS. The time delay compensation block implemented in the PSS class of PSAT has the form of

$$C_{TD}(s) = K_{td}\frac{T_1 s + 1}{T_2 s + 1} \tag{4}$$

where K_{td}, T_1, and T_2 are the parameters designed to compensate for the delay. Responses after the disturbance implementing PSS with delay compensation are compared and illustrated in Fig. 14. Comparing the response with delay compensation (in magenta) to the response with no delay (in red) in Fig. 13, the responses are not the same. The delay compensation cannot restore the responses completely but help in maintaining an acceptable damping performance (with smaller overshoot).

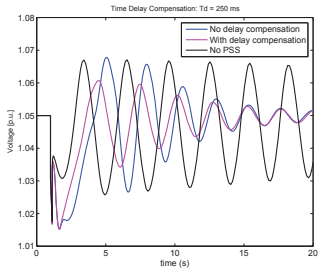

Fig. 14. PSS with Delay Compensation

V. Conclusions

The impact of time delays on frequency- and time-domain responses when using dominant path signals as PSS controller feedback inputs has been illustrated and analyzed in this study. It has been demonstrated that, regardless of the signal of choice, time delays not only result in additional phase compensation requirements but also degrade the controller's damping performance and could destabilize the system (when the time delay is equal to the system's delay margin). Additionally, the impact of time delays are different for each types of feedback signals depending on the signals' open-loop observability or network modeshape.

Important relationships between network modeshape and properties of the dominant path signals subject to time delays have also been summarized. Signals' network modeshapes are proportional to their gains measured at the inter-area frequency, which relates to their damping capacity. The closer (electrically) the signal to the controller, the smaller phase compensation that is required. Although using the dominant path signals as feedback inputs could yield better damping performance, they depend on the maximum delay allowed by the stability limit of the control loop; the larger the network modeshape a signal has, the smaller the delay margin is.

When considering to implement adaptive signal selection in damping controls, one must taken into account simultaneously the network modeshape properties of the signals as well as the control location while delay margin can serve as a design parameter that the ICT system must meet.

Due to space limitations, applications on large power systems will be presented in future publications. Furthermore, the analysis of varying (stochastic) time delays is limited by the simulation software. The analysis of stochastic time-varying delays require the simulation of a hybrid automata. This can be approached with a unified modeling approach for hybrid systems such as the one described in [12] or with an implicit modeling approach where the time-delay can be modeled using discrete equations and combined with the power system continuous time model. The simulation tool (PSAT) used in this study (and the entirety of power system simulation sofware availabe) does not allow for either of these modeling approaches. However, the implicit approach may be possible to do so using Modelica-based software [13] which currently has been under investigation.

References

[1] J. Bergmans, "Effect of Loop Delay on Phase Margin of First-Order and Second-Order Control Loops," *IEEE Transactions on Circuits and Systems-II: Express Briefs*, vol. 52, no. 10, pp. 621–625, October 2005.

[2] J. H. Chow, J. J. Sanchez-Gasca, H. Ren, and S. Wang, "Power System Damping Controller Design Using Multiple Input Signals," *IEEE Control Systems Magazine*, pp. 82–90, August 2000.

[3] H. Wu, K. S. Tsakalis, and G. T. Heydt, "Evaluation of Time Delay Effects to Wide-Area Power System Stabilizer Design," *IEEE Transactions on Power Systems*, vol. 19, no. 4, pp. 1935–1941, November 2004.

[4] Y. Chompoobutrgool and L. Vanfretti, "Identification of Power System Dominant Inter-Area Oscillation Paths," *IEEE Transactions on Power Systems*, vol. PP, no. 99, 2012, available online.

[5] L. Vanfretti, Y. Chompoobutrgool, and J. Chow, *Power System Coherency and Model Reduction*. London: Springer, 2013, ch. 10 Interarea Mode Analysis for Large Power Systems Using Synchrophasor Data.

[6] Y. Chompoobutrgool and L. Vanfretti, "A Fundamental Study on Damping Control Design using PMU Signals from Dominant Inter-Area Oscillation Paths," in *North American Power Symposium (NAPS), 2012*, September 2012, pp. "1–6".

[7] Y. Zhang and A. Bose, "PMU-based wide-area damping control system design," *IEEE Power and Energy Society General Meeting*, 2012.

[8] F. Milano, L. Vanfretti, and J. Morataya, "An Open Source Power System Virtual Laboratory: The PSAT Case and Experience," *IEEE Transactions on Education*, vol. 51, no. 1, pp. 17–23, February 2008.

[9] W. Li, L. Vanfretti, and Y. Chompoobutrgool, "Development and implementation of hydro turbine and governor models in a free and open source software package," *Simulation Modelling Practice and Theory*, vol. 24, pp. 84–102, 2012.

[10] A. Packard, "Ch. 14 Robustness Margin," University Lecture, 2005. [Online]. Available: http://jagger.berkeley.edu/~pack/me132/Section14.pdf

[11] G. Franklin, J. Powell, and A. Emami-Naeini, *Feedback Control of Dynamic Systems*. Prentice Hall, 2002.

[12] J. J. Nutaro, *Building Software for Simulation: Theory and Algorithms, with Applications in C++*. Hoboken, New Jersey: John Wiley & Sons, Inc., 2011.

[13] M. Otter, B. Thiele, and H. Elmqvist, "A Library for Synchronous Control Systems in Modelica," in *Proceedings of the 9th International Modelica Conference*, Munich, Germany, September 2012, pp. 27–36.